

# **Cortical Acetylcholine Levels Correlate with Neurophysiologic Complexity during Subanesthetic Ketamine and Nitrous Oxide Exposure in Rats**

Michael A. Brito,<sup>1,2,3</sup> Duan Li,<sup>1,3</sup> Christopher W. Fields,<sup>1</sup> Chloe Rybicki-Kler,<sup>1</sup> Jon G. Dean,<sup>1,3,4</sup>  
Tiecheng Liu,<sup>1</sup> George A. Mashour,<sup>1,2,3</sup> Dinesh Pal,<sup>1,2,3,4</sup>

<sup>1</sup>Department of Anesthesiology, University of Michigan, 7433 Medical Science Building I, 1150 West Medical Center Drive, Ann Arbor, MI 48109-5615, USA

<sup>2</sup>Neuroscience Graduate Program, University of Michigan, 4137 Undergraduate Science Building, 204 Washtenaw Avenue, Ann Arbor, MI 48109-2215, USA

<sup>3</sup>Center for Consciousness Science, University of Michigan, Ann Arbor, MI 48109, USA

<sup>4</sup>Department of Molecular and Integrative Physiology, University of Michigan, 7744 Medical Science Building II, 1137 East Catherine Street, Ann Arbor, MI 48109-5622, USA

## **To whom correspondence should be addressed:**

Dinesh Pal, Ph.D.  
Assistant Professor  
Department of Anesthesiology  
Department of Molecular and Integrative Physiology  
Neuroscience Graduate program  
Center for Consciousness Science  
University of Michigan  
1150 W Med Ctr Dr, 7433 Med Sci 1  
Ann Arbor, Michigan 48109  
Ph: 734-615-0234  
FAX: 734-764-9332  
[dineshp@med.umich.edu](mailto:dineshp@med.umich.edu)  
ORCID No: 0000-0003-1239-5057

## **Surgical Procedures**

Rats (n = 24, 12 male, 12 female) were anesthetized with 4–5% isoflurane in 100% oxygen in an anesthesia induction chamber, were re-positioned to breathe through a nose cone (Model 906, David Kopf Instruments, Tujunga, CA), and immobilized in a stereotaxic frame using blunt ear bars (Model 963, David Kopf Instruments, Tujunga, CA). After positioning in the stereotaxic instrument, the isoflurane concentration was titrated to the loss of the pedal and palpebral reflex. The concentration of isoflurane was monitored throughout the surgery using an anesthetic agent analyzer (Capnomac Ultima, Datex Medical Instrumentation, Tewksbury, MA). Body temperature was maintained at 37 °C using a far-infrared heating pad (RT-0502, Kent Scientific, Torrington, CT) coupled to a rectal probe (Model 7001H, Physitemp Instruments, Clifton, NJ). Subcutaneous buprenorphine (Buprenex, Par Pharmaceutical, Chestnut Ridge, NY; NDC 42023-179-05) was used as a pre- (0.01 mg/kg) and postsurgical (0.03 mg/kg, every 8-12 h for 48 h) analgesic. A pre-surgical subcutaneous dose of carprofen (5 mg/kg) (Zoetis; NADA #141-199) was administered to supplement surgical and postsurgical analgesia achieved via buprenorphine. A single pre-surgical dose of cefazolin (20 mg/kg, subcutaneous) (West-Ward-Pharmaceutical, Eatontown, NJ; NDC 0143-9924-90) was used as a prophylactic antibiotic.

Burr holes (30) were drilled across the skull and stainless-steel screw electrodes (B000FN89DM, Small Parts, Logansport, IN) were implanted in a regularly spaced montage (anterior-posterior coordinates: 4 mm anterior to 10 mm posterior relative to bregma, 8 rows of electrodes; medial-lateral coordinates: 2 mm to 4.5 mm relative to bregma, 4 electrodes in first 7 rows, 2 in the last row, **Supplementary Figure 1**) to allow for the recording of high-density intracranial EEG. A screw electrode was implanted over the nasal sinus to serve as the reference electrode, while another was implanted over the cerebellum as a ground electrode. CMA 11 microdialysis guide

cannulae (8309018, Harvard Apparatus, Holliston, MA) were implanted 1.0 mm above the prefrontal prelimbic cortex (Bregma, anterior: 3.24 mm, mediolateral: 0.5 mm, ventral: 3 mm) or 2.0 mm above the somatosensory barrel field region of the parietal cortex (Bregma, posterior 3.48, mediolateral 2.6 mm, ventral 2.5 mm, 40° angle)<sup>1</sup> to allow for simultaneous multi-site measurement of cortical acetylcholine levels. In a subset of rats (n = 12, 6 male, 6 female), an indwelling catheter (MRE-040, Micro-Renathane tubing, Braintree Scientific, Braintree, MA, USA) was surgically positioned into the jugular vein to allow for intravenous infusion of ketamine (Ketalar, Par Pharmaceutical, Chesnut Ridge, NY; NDC 42023-115-10).

### **Quantification of cortical acetylcholine in prefrontal and parietal cortices**

CMA/11 microdialysis probes (CMA Microdialysis, Harvard Apparatus, Holliston, MA, USA) were inserted into the prefrontal cortex (1 mm cuprophane membrane, 0.24 mm diameter, 6 kDa membrane cutoff, 8309581) and somatosensory barrel field region of parietal cortex (2 mm cuprophane membrane, 0.24 mm diameter, 6 kDa membrane cutoff, 8309582). The probes were connected to a microsyringe pump (Model CMA/400, CMA Microdialysis, Harvard Apparatus, Holliston, MA, USA) and were continuously perfused with artificial cerebrospinal fluid (aCSF; 145 mM NaCl, Sigma Aldrich: S9888; 2.68 mM KCl, Sigma Aldrich: P9333; 1.40 mM CaCl<sub>2</sub> • 2H<sub>2</sub>O, Sigma Aldrich: C8106; 1.01 mM MgSO<sub>4</sub> • 7H<sub>2</sub>O, Sigma Aldrich: 63140; 1.55 mM Na<sub>2</sub>HPO<sub>4</sub>, Sigma Aldrich: S5136; 0.45 mM NaH<sub>2</sub>PO<sub>4</sub> • H<sub>2</sub>O, Sigma Aldrich: 52074; 10 μM neostigmine, Sigma Aldrich: N2001; pH = 7.4) at a rate of 2 μL/min, allowing for sample collection at a volume of 25 μL in epochs of 12.5 mins. To rule out the possibility of any potential change in probe membrane properties affecting the neurochemical analysis, we compared the recovery profile of the probes before and after the experiments using 3 pmol acetylcholine/choline standard.

Acetylcholine concentration was quantified via high-performance liquid chromatography (HPLC) coupled to an electrochemical detector (HTEC-510, Amuza Inc. San Diego, CA, USA). Mobile phase was perfused through the system at 175  $\mu\text{L}/\text{min}$  and had a composition of 49.95 mM  $\text{KHCO}_3$  (Sigma Aldrich: 237205) ;148.72  $\mu\text{M}$   $\text{Na}_2\text{EDTA} \cdot 2\text{H}_2\text{O}$  (Amuza/Dojindo: 111.114.91), and 1.23 mM decanesulfonate sodium salt (Amuza/TCI: 900.061.00) per 1 liter of ultrapure HPLC-grade water (Milli-Q, EMD Millipore, Burlington, MA, USA).

We injected 20  $\mu\text{L}$  from each microdialysis sample into a 50  $\mu\text{L}$  sample loop connected to a polymer-based reverse phase separation column (AC-GEL, 2.0 mm  $\varnothing$  x 150 mm, Amuza Inc., San Diego, CA, USA), allowing for the separation of acetylcholine and choline in the biological samples. Acetylcholine and choline are then broken down to produce hydrogen peroxide proportional to their relative concentrations (AC-ENZYMPAK II ACh enzyme reactor, 1 mm x 4 mm, Amuza Inc., San Diego, CA, USA). Hydrogen peroxide is oxidized at the platinum electrode surface (WE-PT platinum electrode, RE-500 Ag/Cl reference electrode, applied potential: +450 mV; Amuza Inc., San Diego, CA) and the generated current is detected by the electrochemical detector. A seven-point acetylcholine/choline standard curve (0.05 – 1.0 pmol) was generated prior to the start of each experiment, as outlined in previous experiments from our laboratory<sup>2-4</sup>.

### **EEG data acquisition**

Monopolar EEG data were acquired using a 32-channel headstage (Cereplex  $\mu$ , Blackrock Microsystems, Salt Lake City, UT). The signals were then digitized at 1 kHz and bandpass filtered between 0.1-500 Hz using a Cereplex Direct system paired with the Cereplex Direct Software Suite (Blackrock Microsystems, Salt Lake City, UT). Raw EEG signals were imported into MATLAB (version 2020b; MathWorks, Inc.; Natick, MA). Data segments with obvious

noise or artifacts were identified and removed by visual inspection of both the raw waveform and spectrogram of the EEG signals. Prior to analyses, the EEG signals were detrended using a local linear regression method with a 10 s window at a 2 s step size in Chronux analysis software <sup>4</sup>, and subsequently lowpass filtered at 175 Hz via fifth-order Butterworth filter.

### **Frontoparietal directed connectivity: normalized symbolic transfer entropy analysis**

To assess directed connectivity between frontal and parietal cortices, we used normalized symbolic transfer entropy (NSTE), which is an information theoretic measure. Transfer entropy has been proposed as a surrogate measure to estimate the directional exchange of information between two signals, such as those recorded from neural data <sup>5</sup>. More specifically, NSTE is a non-parametric, nonlinear, and model-free means by which one can approximate the degree of statistical dependence between the EEG signals recorded from disparate brain regions. The precise method used is outlined in detail in a number of previous human <sup>6-8</sup> and rat studies<sup>3,10,11</sup> from our laboratory.

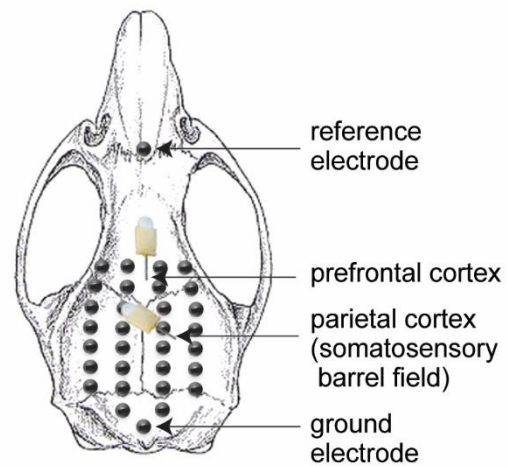
We used EEG data from ipsilateral frontal and parietal channels to assess feedback (frontal-to-parietal) and feedforward (parietal-to-frontal) connectivity before, during, and after subanesthetic ketamine or nitrous oxide administration. We focused on changes in directed connectivity in three gamma bandwidths: low gamma (25-55 Hz), mid gamma (85-125 Hz), and high gamma (125-175 Hz), as gamma oscillations have been implicated in arousal <sup>9</sup> and previous studies from our laboratory have illustrated directed frontoparietal connectivity in high gamma bands to be a correlate of wakefulness.<sup>3,10,11</sup> We used a fourth-order Butterworth filter (butter.m and filtfilt.m, MATLAB Signal Processing Toolbox) to filter the respective gamma bandwidths of interest from the raw EEG signal and then segmented the filtered signal into non-overlapping 10 s windows. The calculation of NSTE is contingent upon three parameters: the embedding

dimension, time delay, and prediction time. We set the embedding dimension at 3 across all analyses. The time delay was set at 5 (10 ms), 2 (4 ms), and 1 (2 ms) for the low, mid, and high gamma bandwidths, respectively. The prediction time was set by searching values between 1 and 50 (corresponding to 2–100 ms) and selecting the value that yielded maximum normalized symbolic transfer entropy in the feedback (frontal-to-parietal) and feedforward (parietal-to-frontal) directions.

### References:

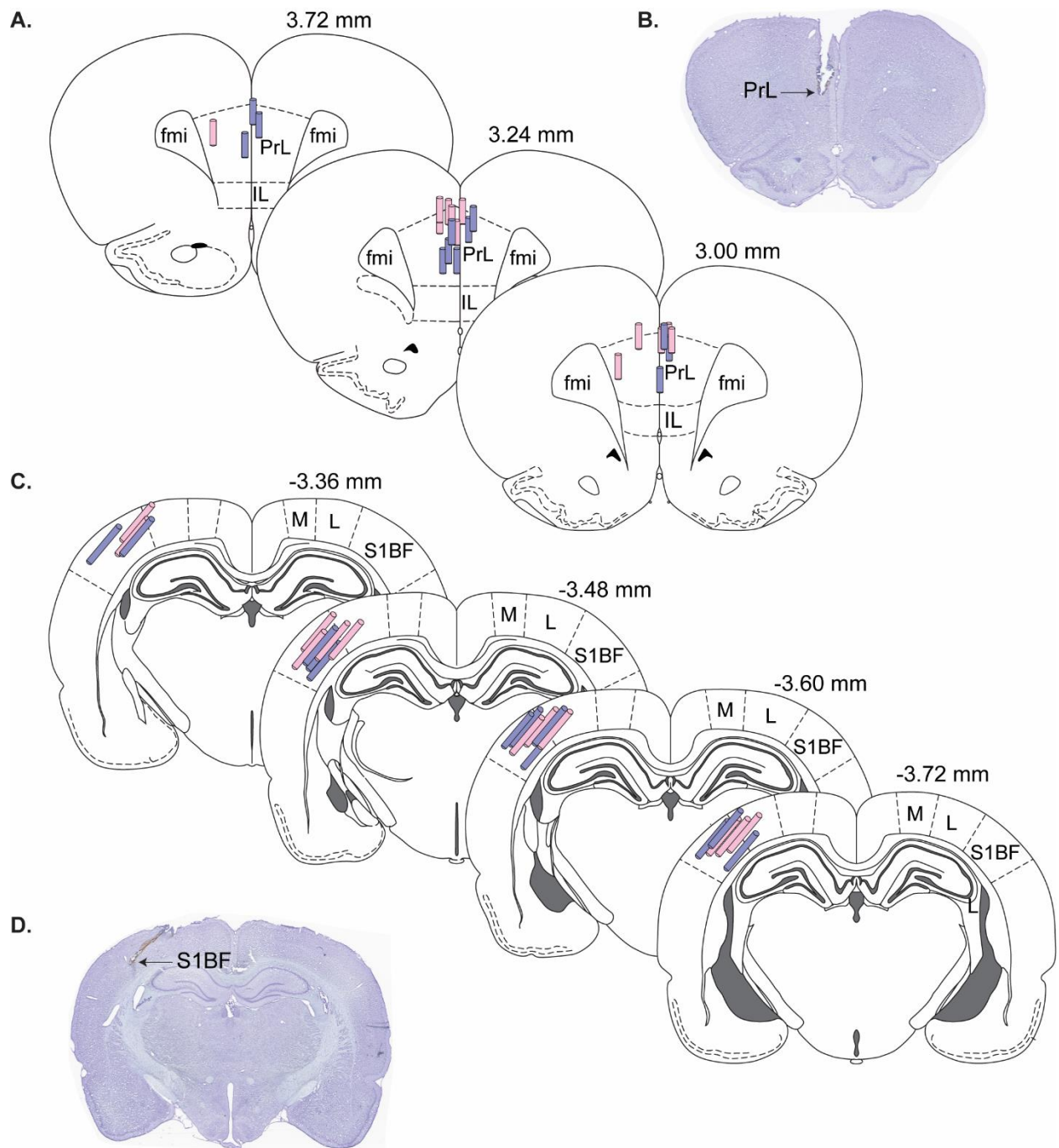
1. Paxinos, G. and Watson C. (2007) *The Rat Brain in Stereotaxic Coordinates*. Academic Press, London.
2. Pal D, Hambrecht-Wiedbusch VS, Silverstein BH, Mashour GA. Electroencephalographic coherence and cortical acetylcholine during ketamine-induced unconsciousness. *Br J Anaesth* 2015;114:979–89.
3. Pal D, Silverstein BH, Lee H, Mashour GA. Neural Correlates of Wakefulness, Sleep, and General Anesthesia: An Experimental Study in Rat. *Anesthesiology* 2016;125:929–42.
4. Pal D, Dean JG, Liu T, et al. Differential Role of Prefrontal and Parietal Cortices in Controlling Level of Consciousness. *Curr Biol* 2018;28:2145-2152.e5.
5. Bokil H, Andrews P, Kulkarni JE, Mehta S, Mitra P. Chronux: A Platform for Analyzing Neural Signals. *J Neurosci Methods* 2010;192:146–51.
6. McAuliffe J. The new math of EEG: Symbolic transfer entropy, the effects of dimension. *Clin Neurophysiol* 2014;125:e17.

7. Ku S-W, Lee U, Noh G-J, Jun I-G, Mashour GA. Preferential Inhibition of Frontal-to-Parietal Feedback Connectivity Is a Neurophysiologic Correlate of General Anesthesia in Surgical Patients. *PLoS ONE* 2011;6:e25155.
8. Lee U, Kim S, Noh G-J, Choi B-M, Hwang E, Mashour GA. The directionality and functional organization of frontoparietal connectivity during consciousness and anesthesia in humans. *Conscious Cogn* 2009;18:1069–78.
9. Lee U, Ku S, Noh G, Baek S, Choi B, Mashour GA. Disruption of Frontal–Parietal Communication by Ketamine, Propofol, and Sevoflurane: *Anesthesiology* 2013;118:1264–75.
10. Borjigin J, Lee U, Liu T, et al. Surge of neurophysiological coherence and connectivity in the dying brain. *Proc Natl Acad Sci* 2013;110:14432–7.
11. Pal D, Li D, Dean JG, et al. Level of Consciousness Is Dissociable from Electroencephalographic Measures of Cortical Connectivity, Slow Oscillations, and Complexity. *J Neurosci* 2020;40:605–18.



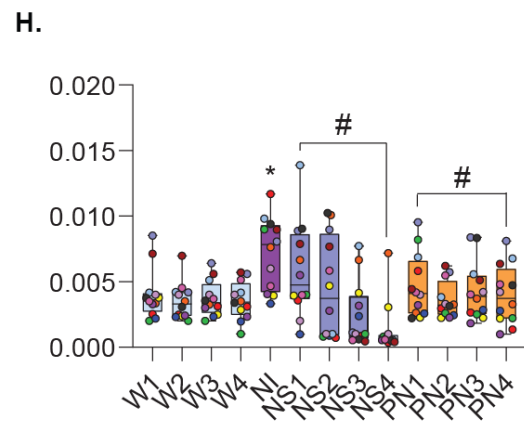
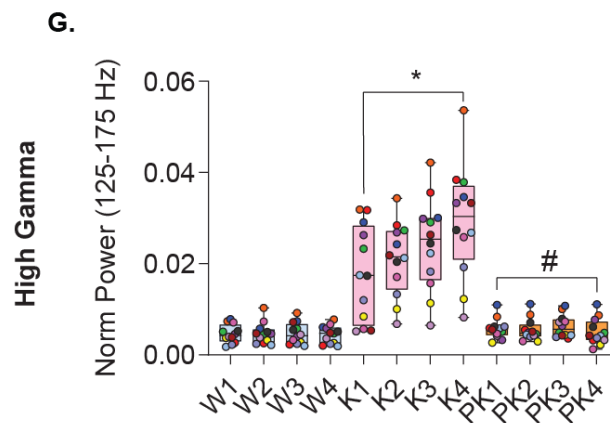
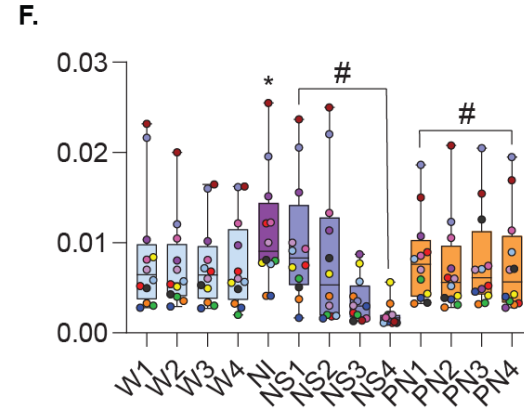
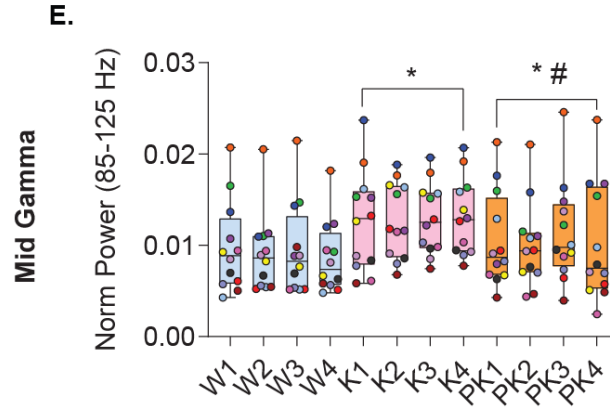
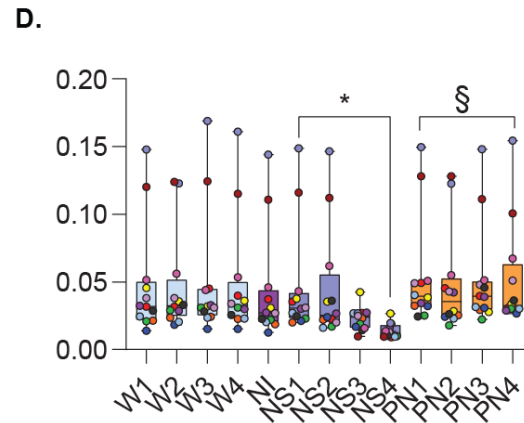
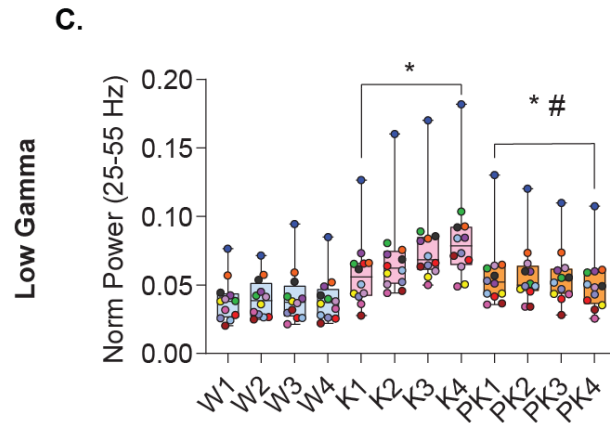
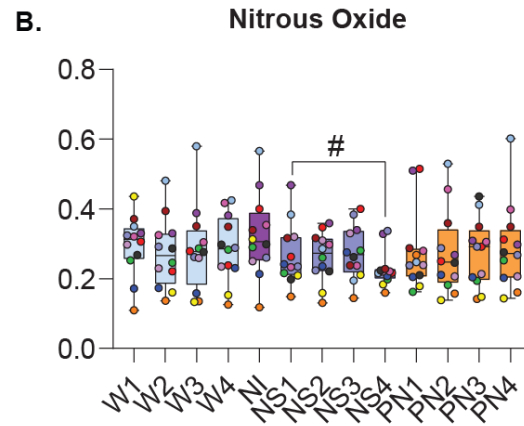
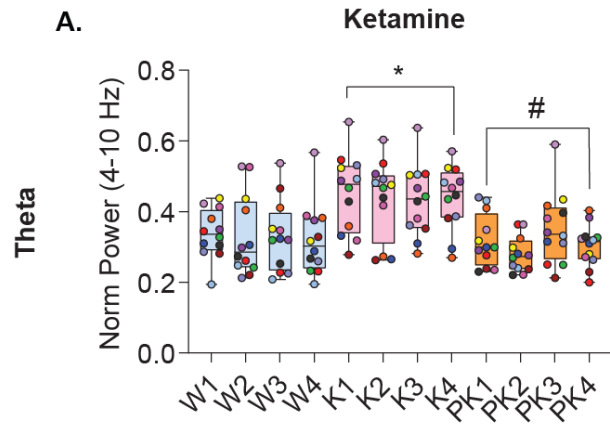
**Supplemental Digital Content, Figure 1:** Schematic showing the EEG montage (30 screw electrodes) to record high-density intracranial EEG and placement of microdialysis probes in prefrontal cortex and somatosensory barrel field region of the parietal cortex. A single screw electrode on the nasal sinus served as a reference while another electrode over the cerebellum served as the ground.





**Supplemental Digital Content, Figure 2:** Histological verification of microdialysis probe placement in prefrontal and parietal cortices. Stereotaxic maps from the rat brain atlas (Paxinos and Watson, 2006) show the location of microdialysis probes in the prelimbic (PrL) region of

prefrontal cortex and somatosensory barrel field (S1BF) region of parietal cortex. Pink cylinders (**A, C**) represent probes from ketamine experiments while purple cylinders represent probes from nitrous oxide experiments (**A, C**). **B** and **D** show cresyl violet-stained representative coronal brain sections (40  $\mu\text{m}$ ) through prefrontal cortex and parietal cortex, respectively. fmi – forceps minor corpus callosum, IL – infralimbic area, L – lateral parietal association cortex, M – medial parietal association cortex. The numbers on top right of the stereotaxic maps show the distance from Bregma; positive numbers are anterior to Bregma while negative numbers are posterior to Bregma.



**Supplemental Digital Content, Figure 3:** Power spectral changes before, during, and after subanesthetic ketamine infusion or nitrous oxide exposure. Normalized power (discrete Fourier transform with 10 s segment size, a 2 s window size, and 80% overlap) was calculated as the proportion of a specific frequency power in the total power over all frequency bands averaged across all channels. Subanesthetic ketamine infusion (K) induced sustained increases in theta power (4-10 Hz) as compared to the baseline wake state (W), while theta power during nitrous oxide exposure did not significantly differ from the wake state at either induction (NI) or sedation (NS) periods (**A, B**). Subanesthetic ketamine infusion induced sustained increases in low gamma power (25-55 Hz), increasing progressively as a function of the length of the infusion (**C**). As compared to the wake state, nitrous oxide induction period was not characterized by a significant change in low gamma power but was attenuated during the following 50 minutes of sedation period (**D**). In the mid gamma bandwidth (85-125 Hz), subanesthetic ketamine was found to enhance power for the entirety of the infusion period as compared to the wake state (**E**). In contrast, nitrous oxide produced state-dependent effects on mid gamma power when compared with wakefulness; there was an increase in power during the induction period, which was significantly attenuated during the sedation period (**F**). Subanesthetic ketamine infusion promoted a progressive increase in power in the high gamma bandwidth (125-175 Hz) compared to the wake state (**G**), while nitrous oxide was found to exert state-dependent effects – increase in high gamma power during induction period but decrease during sedation period (**H**). The statistical comparisons are shown at  $P < .05$ . K – subanesthetic ketamine infusion, NI – nitrous oxide induction, NS – nitrous oxide sedation, PK – postketamine recovery, PN – postnitrous oxide, W – wake. \*Significant compared to wake, #significant

compared to subanesthetic ketamine infusion or nitrous oxide induction, §significant compared to nitrous oxide sedation.

**Supplemental Digital Content, Table 1** Cortical acetylcholine before, during, and after intravenous infusion of subanesthetic ketamine.

<b>Prefrontal Cortex</b>			
<b>Wake</b>	<b>Ketamine infusion</b>	<b>Postketamine recovery</b>	<b>F-Statistic</b>
0.5 ± 0.09 [0.42 - 0.58]	0.87 ± 0.15 [0.79 - 0.95] * <i>P</i> < .001	0.61 ± 0.12 [0.53 - 0.68] * <i>P</i> = .002 # <i>P</i> < .001	F(2,130)=82.92 * <i>P</i> < .001
<b>Parietal Cortex</b>			
<b>Wake</b>	<b>Ketamine infusion</b>	<b>Postketamine recovery</b>	<b>F-Statistic</b>
0.72 ± 0.17 [0.55 - 0.88]	1.59 ± 0.45 [1.43 - 1.75] * <i>P</i> < .001	0.88 ± 0.15 [0.72 - 1.04] * <i>P</i> = .03 # <i>P</i> < .001	F(2,130)=106.46 * <i>P</i> < .001

Data are shown as mean ± standard deviation with 95% confidence interval in brackets.

\*Compared to Wake, #compared to Ketamine infusion.

**Supplemental Digital Content, Table 2** Cortical acetylcholine before, during, and after nitrous oxide administration.

<b>Prefrontal Cortex</b>				
<b>Wake</b>	<b>Nitrous induction</b>	<b>Nitrous sedation</b>	<b>Postnitrous recovery</b>	<b>F-Statistic</b>
0.34 ± 0.11 [0.28 - 0.42]	0.54 ± 0.22 [0.46 - 0.61] <i>*P</i> < .001	0.27 ± 0.11 [0.20 - 0.33] <i>*P</i> < .001 # <i>P</i> < .001	0.37 ± 0.11 [0.31 - 0.44] <i>*P</i> = .247 # <i>P</i> < .001 § <i>P</i> < .001	F(3,141)=45.13 <i>*P</i> < .001
<b>Parietal Cortex</b>				
<b>Wake</b>	<b>Nitrous induction</b>	<b>Nitrous sedation</b>	<b>Postnitrous recovery</b>	<b>F-Statistic</b>
0.5 ± 0.09 [0.45 - 0.55]	0.71 ± 0.19 [0.64 - 0.83] <i>*P</i> < .001	0.37 ± 0.11 [0.32 - 0.42] <i>*P</i> < .001 # <i>P</i> < .001	0.50 ± 0.11 [0.45 - 0.55] <i>*P</i> = 1 # <i>P</i> < .001 § <i>P</i> < .001	F(3,141)=52.72 <i>*P</i> < .001

Data are shown as mean ± standard deviation with 95% confidence interval in brackets.

\*Compared to Wake, #compared to Nitrous induction, §compared to Nitrous sedation.

**Supplemental Digital Content, Table 3** Normalized Lempel-Ziv complexity before, during, and after intravenous infusion of subanesthetic ketamine.

<b>Wake</b>	<b>Ketamine infusion</b>	<b>Postketamine recovery</b>	<b>F-Statistic</b>
0.983 ± 0.006 [0.979 - 0.986]	0.995 ± 0.004 [0.992 - 0.998] * <i>P</i> < .001	0.984 ± 0.005 [0.981 - 0.987] * <i>P</i> = .7 # <i>P</i> < .001	F(2,130)=58.4 * <i>P</i> < .001

Data are shown as mean ± standard deviation with 95% confidence interval in brackets.

\*Compared to Wake, #compared to Ketamine infusion.



**Supplemental Digital Content, Table 4** Normalized Lempel-Ziv complexity before, during, and after nitrous oxide administration.

<b>Wake</b>	<b>Nitrous induction</b>	<b>Nitrous sedation</b>	<b>Postnitrous recovery</b>	<b>F-Statistic</b>
0.979 ± 0.007 [0.973 - 0.986]	0.994 ± 0.004 [0.982 - 1.006] <i>*P</i> = .04	0.953 ± 0.012 [0.947 - 0.960] <i>*P</i> < .001 <i>#P</i> < .001	0.981 ± 0.008 [0.974 - 0.987] <i>*P</i> = 1 <i>#P</i> = .09 <i>§P</i> < .001	F(3,141)=31.9 <i>*P</i> < .001

Data are shown as mean ± standard deviation with 95% confidence interval in brackets.

*\**Compared to Wake, *#*compared to Nitrous induction, *§*compared to Nitrous sedation.

**Supplemental Digital Content, Table 5** Directed frontoparietal connectivity in gamma bandwidths before, during, and after intravenous infusion of subanesthetic ketamine.

<b>Feedback Connectivity</b>				
<b>Frequency (Hz)</b>	<b>Wake</b>	<b>Ketamine infusion</b>	<b>Postketamine recovery</b>	<b>F-Statistic</b>
<b>low <math>\gamma</math></b> (25–55)	0.009 $\pm$ 0.003 [0.008 - 0.011]	0.008 $\pm$ 0.002 [0.006 - 0.01] * <i>P</i> < .001	0.009 $\pm$ 0.002 [0.007 - 0.01] * <i>P</i> = .08 # <i>P</i> < .001	F(2,130)=23.84 * <i>P</i> < .001
<b>mid <math>\gamma</math></b> (85–125)	0.027 $\pm$ 0.008 [0.023 - 0.030]	0.017 $\pm$ 0.006 [0.013 - 0.020] * <i>P</i> < .001	0.0196 $\pm$ 0.005 [0.016 - 0.023] * <i>P</i> < .001 # <i>P</i> < .001	F(2,130)=120.1 * <i>P</i> < .001
<b>high <math>\gamma</math></b> (125–175)	0.042 $\pm$ 0.008 [0.037 - 0.048]	0.07 $\pm$ 0.013 [0.065 - 0.076] * <i>P</i> < .001	0.041 $\pm$ 0.009 [0.036 - 0.047] * <i>P</i> = 1 # <i>P</i> < .001	F(2,130)=211.5 * <i>P</i> < .001
<b>Feedforward Connectivity</b>				
<b>Frequency (Hz)</b>	<b>Wake</b>	<b>Ketamine infusion</b>	<b>Postketamine recovery</b>	<b>F-Statistic</b>
<b>low <math>\gamma</math></b> (25–55)	0.008 $\pm$ 0.002 [0.006 - 0.009]	0.006 $\pm$ 0.002 [0.005 - 0.008] * <i>P</i> < .001	0.007 $\pm$ 0.002 [0.006 - 0.009] * <i>P</i> = .13 # <i>P</i> < .001	F(2,130)=36.67 * <i>P</i> < .001
<b>mid <math>\gamma</math></b> (85–125)	0.03 $\pm$ 0.006 [0.026 - 0.034]	0.021 $\pm$ 0.007 [0.017 - 0.025] * <i>P</i> < .001	0.022 $\pm$ 0.005 [0.018 - 0.026] * <i>P</i> = .001 # <i>P</i> = .1	F(2,130)=130.01 * <i>P</i> < .001
<b>high <math>\gamma</math></b> (125–175)	0.045 $\pm$ 0.01 [0.037 - 0.054]	0.08 $\pm$ 0.021 [0.074 - 0.091] * <i>P</i> < .001	0.044 $\pm$ 0.012 [0.036 - 0.053] * <i>P</i> = .796 # <i>P</i> < .001	F(2,130)=205.84 * <i>P</i> < .001

Data are shown as mean  $\pm$  standard deviation with 95% confidence interval in brackets.

\*Compared to Wake, #compared to Ketamine infusion.

**Supplemental Digital Content, Table 6** Directed frontoparietal connectivity in gamma bandwidths before, during, and after nitrous oxide administration.

<b>Feedback Connectivity</b>					
<b>Frequency (Hz)</b>	<b>Wake</b>	<b>Nitrous induction</b>	<b>Nitrous sedation</b>	<b>Postnitrous recovery</b>	<b>F-Statistic</b>
<b>low <math>\gamma</math></b> (25–55)	0.011 $\pm$ 0.003 [0.008 - 0.013]	0.011 $\pm$ 0.004 [0.008 - 0.014] * <i>P</i> = 1	0.0141 $\pm$ 0.008 [0.012 - 0.016] * <i>P</i> < .001 # <i>P</i> = .002	0.011 $\pm$ 0.003 [0.009 - 0.013] * <i>P</i> = 1 # <i>P</i> = 1 § <i>P</i> < .001	F(3,141)=17.98 * <i>P</i> < .001
<b>mid <math>\gamma</math></b> (85–125)	0.023 $\pm$ 0.004 [0.02 - 0.026]	0.03 $\pm$ 0.007 [0.027 - 0.034] * <i>P</i> < .001	0.022 $\pm$ 0.005 [0.019 - 0.025] * <i>P</i> = .66 # <i>P</i> < .001	0.021 $\pm$ 0.004 [0.018 - 0.024] * <i>P</i> < .04 # <i>P</i> < .001 § <i>P</i> = .4	F(3,141)=22.6 * <i>P</i> < .001
<b>high <math>\gamma</math></b> (125–175)	0.038 $\pm$ 0.015 [0.028 - 0.047]	0.047 $\pm$ 0.019 [0.036 - 0.058] * <i>P</i> < .001	0.037 $\pm$ 0.016 [0.027 - 0.047] * <i>P</i> = .968 # <i>P</i> < .001	0.037 $\pm$ 0.014 [0.028 - 0.047] * <i>P</i> = .968 # <i>P</i> < .001 § <i>P</i> = .999	F(3,141) = 6.46 * <i>P</i> < .001
<b>Feedforward Connectivity</b>					
<b>Frequency (Hz)</b>	<b>Wake</b>	<b>Nitrous induction</b>	<b>Nitrous sedation</b>	<b>Postnitrous recovery</b>	<b>F-Statistic</b>
<b>low <math>\gamma</math></b> (25–55)	0.09 $\pm$ 0.003 [0.007 - 0.010]	0.009 $\pm$ 0.004 [0.008 - 0.011] * <i>P</i> = 1	0.012 $\pm$ 0.008 [0.01 - 0.013] * <i>P</i> < .001 # <i>P</i> = .002	0.009 $\pm$ 0.003 [0.008 - 0.011] * <i>P</i> = 1 # <i>P</i> = 1 § <i>P</i> < .001	F(3,141)=17.98 * <i>P</i> < .001
<b>mid <math>\gamma</math></b> (85–125)	0.026 $\pm$ 0.006 [0.023 - 0.031]	0.034 $\pm$ 0.009 [0.03 - 0.039] * <i>P</i> < .001	0.024 $\pm$ 0.005 [0.021 - 0.029] * <i>P</i> = .05 # <i>P</i> < .001	0.025 $\pm$ 0.006 [0.021 - 0.029] * <i>P</i> = .06 # <i>P</i> < .001 § <i>P</i> = 1	F(3,141)=22.58 * <i>P</i> < .001
<b>high <math>\gamma</math></b> (125–175)	0.040 $\pm$ 0.016 [0.03 - 0.05]	0.056 $\pm$ 0.025 [0.039 - 0.07] * <i>P</i> < .001	0.042 $\pm$ 0.023 [0.03 - 0.054] * <i>P</i> = .85 # <i>P</i> < .001	0.039 $\pm$ 0.015 [0.028 - 0.052] * <i>P</i> = 1 # <i>P</i> < .001 § <i>P</i> = .72	F(3,141) = 7.85 * <i>P</i> < .001

Data are shown as mean  $\pm$  standard deviation with 95% confidence interval in brackets.

\*Compared to Wake, #compared to Nitrous induction, §compared to Nitrous sedation.

**Supplemental Digital Content, Table 7** Correlation between changes in cortical acetylcholine and directed frontoparietal connectivity in gamma bandwidths after intravenous infusion of subanesthetic ketamine.

Frequency (Hz)	Prefrontal acetylcholine		Parietal acetylcholine	
	Feedback connectivity	Feedforward connectivity	Feedback connectivity	Feedforward connectivity
<b>low <math>\gamma</math></b> (25–55)	CW $r = -0.21$ [-0.54 – 0.11] $P = .18$	CW $r = -0.26$ [-0.56 – 0.03] $P = .08$	CW $r = -0.18$ [-0.43 – 0.06] $P = .14$	CW $r = -0.20$ [-0.44 – 0.04] $P = .09$
<b>mid <math>\gamma</math></b> (85–125)	CW $r = -0.47$ [-0.67 – -0.27] $*P < .001$	CW $r = -0.40$ [-0.60 – -0.19] $*P < .001$	CW $r = -0.48$ [-0.73 – -0.23] $*P < .001$	CW $r = -0.43$ [-0.72 – -0.15] $*P < .01$
<b>high <math>\gamma</math></b> (125–175)	CW $r = 0.54$ [0.35 – 0.72] $*P < .001$	CW $r = 0.48$ [0.25 – 0.70] $*P < .001$	CW $r = 0.64$ [0.54 – 0.74] $*P < .001$	CW $r = 0.58$ [0.46 – 0.70] $*P < .001$

Data are shown as the cluster-weighted marginal correlation coefficient with 95% confidence interval in brackets.

\*Significant correlation.

**Supplemental Digital Content, Table 8** Correlation between changes in cortical acetylcholine and directed frontoparietal connectivity in gamma bandwidths in the nitrous oxide group.

Frequency (Hz)	Prefrontal acetylcholine		Parietal acetylcholine	
	Feedback connectivity	Feedforward connectivity	Feedback connectivity	Feedforward connectivity
<b>low <math>\gamma</math></b> (25–55)	CW $r = 0.13$ [-0.11 – 0.37] $P = .28$	CW $r = 0.11$ [-0.11 – 0.34] $P = .32$	CW $r = -0.11$ [-0.29 – 0.08] $P = .1$	CW $r = -0.07$ [-0.229 – 0.093] $P = .25$
<b>mid <math>\gamma</math></b> (85–125)	CW $r = 0.18$ [-0.03 – 0.40] $P = .09$	CW $r = 0.35$ [0.17 – 0.53] $*P < .001$	CW $r = 0.23$ [0.02 – 0.42] $*P < .05$	CW $r = 0.25$ [0.01 – 0.48] $*P < .05$
<b>high <math>\gamma</math></b> (125–175)	CW $r = 0.42$ [0.17 – 0.68] $*P < .01$	CW $r = 0.46$ [0.20 – 0.71] $*P < .001$	CW $r = 0.16$ [-0.18 – 0.49] $P = .36$	CW $r = 0.20$ [-0.13 – 0.54] $P = .23$

Data are shown as the cluster-weighted marginal correlation coefficient with 95% confidence interval in brackets.

\*Significant correlation.

**Supplemental Digital Content, Table Legends:**

**Supplemental Digital Content, Table 1:** Cortical acetylcholine before, during, and after intravenous subanesthetic ketamine infusion.

Data are shown as mean  $\pm$  standard deviation of the mean with the 95% confidence interval in brackets. \*Compared to baseline wake state, #compared to subanesthetic ketamine infusion.

**Supplemental Digital Content, Table 2:** Cortical acetylcholine before, during, and after subanesthetic nitrous oxide exposure.

Data are shown as mean  $\pm$  standard deviation of the mean with the 95% confidence interval in brackets. \*Compared to baseline wake state, #compared to nitrous oxide induction, §compared to nitrous oxide sedation.

**Supplemental Digital Content, Table 3:** Normalized Lempel-Ziv complexity before, during, and after intravenous subanesthetic ketamine infusion.

Data are shown as mean  $\pm$  standard deviation of the mean with the 95% confidence interval in brackets. \*Compared to baseline wake state, # subanesthetic ketamine infusion.

**Supplemental Digital Content, Table 4:** Normalized Lempel-Ziv complexity before, during, and after subanesthetic nitrous oxide exposure.

Data are shown as mean  $\pm$  standard deviation of the mean with the 95% confidence interval in brackets. \*Compared to baseline wake state, #compared to nitrous oxide induction, §compared to nitrous oxide sedation.

**Supplemental Digital Content, Table 5:** Normalized symbolic transfer entropy in gamma bandwidths before, during, and after intravenous subanesthetic ketamine infusion.

Data are shown as mean  $\pm$  standard deviation of the mean with the 95% confidence interval in brackets. \*Compared to baseline wake state, #compared to subanesthetic ketamine infusion.

**Supplemental Digital Content, Table 6:** Normalized symbolic transfer entropy in gamma bandwidths before, during, and after subanesthetic nitrous oxide exposure.

Data are shown as mean  $\pm$  standard deviation of the mean with 95% confidence interval in brackets. \*Compared to baseline wake state, #compared to nitrous oxide induction, §compared to nitrous oxide sedation.

**Supplemental Digital Content, Table 7:** Correlation between changes in cortical acetylcholine and directed frontoparietal connectivity in gamma bandwidths after intravenous infusion of subanesthetic ketamine.

Data are shown as the cluster-weighted marginal correlation coefficient with 95% confidence interval in brackets. \*Significant correlation.

**Supplemental Digital Content, Table 8:** Correlation between changes in cortical acetylcholine and directed frontoparietal connectivity in gamma bandwidths in the nitrous oxide group.

Data are shown as the cluster-weighted marginal correlation coefficient with 95% confidence interval in brackets. \*Significant correlation.